RSC Advances

ROYAL SOCIETY OF CHEMISTRY

www.rsc.org/advances

Cite this: DOI: 10.1039/c0xx00000x

www.rsc.org/xxxxxx

COMMUNICATION

Highly porous, light weight 3D sponge like graphene aerogel for electromagnetic interference shielding applications†

Sweta Singh,[a] Prashant Tripathi,[a] Ashish Bhatnagar,[a] Ch. Ravi Prakash Patel,[a] Avanish Pratap Singh,[b] S. K. Dhawan,[b] Bipin Kumar Gupta[b] and O. N. Srivastava [a,*]

Received (in XXX, XXX) XthXXXXXXXXX 20XX, Accepted Xth XXXXXXXXX 20XX
DOI: 10.1039/b000000x

Here, we report the microwave shielding properties of light weight three dimensional (3D) sponge like graphene aerogel (GA) derived from graphene oxide (GO). GA is a new exotic form of graphene nanosheets, which show improved shielding features as compared to their pristine counterpart. The structural and microstructural characteristics of this new indigenous 3D sponge like graphene aerogel architecture have been probed by XRD, Raman, SEM and TEM/HRTEM. Further, the porosity of this new synthesized structure has been investigated by Brunauer–Ennett–Teller (BET) method, which confirms the high surface area ~ 516 m^2/g with an average pore diameter ~ 2.5 nm. The high surface area and better porosity mediate the key role to improve the EMI shielding effectiveness of GA. Simultaneously, GA nanostructure also enhances the dielectric properties which provide a better alternative for EMI shielding material as compare to GO. This engineered GA exhibit enhanced shielding effectiveness (~ 20.0 dB at 0.20 g in frequency region 12.4 to 18.0 GHz) as compared to conventional GO. Thus, the result of EMI shielding of GA offers a new ingenious nanostructure which can be used as an EMI pollutant quencher for next-generation EMI shielding devices.

In modern era, electromagnetic shielding materials is highly desirable in an attempt to protect the environment from EMI pollutants, which is emanating from most of the electronic devices like TV, computer, mobiles, etc.[1] In the past few years, conventional wisdoms of using EMI shielding materials were based on metal films or plates, but they have their own limitations. These metallic systems are heavy, corrosion prone and have poor processibility.[2-3] Simultaneously, their shielding effectiveness was mainly based on reflection rather absorption, which prevents their applications in various areas, including military and aircraft. This is so since the reflected electromagnetic waves will be received and detected by an adversary's reconnaissance instrument. Therefore, a continuous search is going on to develop novel materials associated with excellent absorption features with the purpose to reduce electromagnetic interference (EMI) in circuits, chips and radiation controllers.[4] Recently, immense attempts have been made in the search of high-performance EMI shielding materials with excellent absorption capability. In this regard, the high-performance EMI shielding material having light weight and flexible in nature; are highly desirable. This is due to its practical applications in various fields like aircraft, aerospace, automobiles and fast-growing next-generation flexible electronics such as portable electronics and wearable devices.[5] Carbon materials such as intercalated graphite,[6] carbon nanotubes (CNTs),[7-8] porous carbon,[9-10] carbon nanopowders,[11] carbon fibres,[12] graphene [13-14] and reduced graphene oxide (RGO)[15] have been recently reported to absorb electromagnetic wave. Now a days, two-dimensional layered materials and their composites[16-19] such as graphene and its derivatives are examined as potential microwave absorbers due to their superior electronic, thermal, and mechanical properties. One of the big advantages of using such nanostructures is its high surface area. It is also established that carbon-based layered materials provide highly efficient microwave absorbers as compared to nanotubes or nanorod like structures.[20]

In recent past, significant improvements have been done on the self-assembly of nanomaterials into 3D forms as hydrogels, aerogels, and some other microporous or mesoporous frameworks.[21] As a consequence of the 3D interconnected carbon skeleton, porous carbons provide tremendous microwave absorption capacity.[22-24] As compared to microporous foams like graphene-polymer microcellular foams[25], microporous aerogels are advantageous in several ways. Due to availability of wide range fabrication processes and ability of pore morphologies to be reduced to less than 100 nm, chemically derived GO based graphene aerogels are exotic 3D graphene structures reported in literature.[26] Intrinsic properties of GA like microporosity, high electrical conductivity and high specific surface area are advantageous in various applications such as hydrogen storage, catalysis, batteries, filtration, insulation, sorbents and supercapacitors.[26] GA with very high specific surface area,

microporosity, very low density and excellent electrical conductivity makes it as a promising 3D material for high-performance EMI shielding applications. Moreover, the high microporosity of GA gives rise to high polarity, which leads to good absorption capacity. This arises due to enhanced dielectric loss because of high polarization and presence of defects in the GA nanostructures. These could make GA as an outstanding material for the next-generation microwave shielding applications.

In this communication, we report a facile method of producing large-scale GA and demonstrate its highly suitable application as EMI shielding materials. The desired microwave shielding properties of light weight (apparent density ~ 75 mg/cm^3, its method of calculation is given in supplementary information) 3D GA depends on its parent material GO, which is used during the synthesis of GA. As prepared GA is a new exotic form of highly porous 3D sponge like architecture of graphene nanosheets, which improves the electronic properties in comparison to parent GO nanosheets and conventional carbon aerogel. Based on GO, resorcinol (R) and formaldehyde (F) as a precursor in the synthesis of 3D cross-linked GA is gaining attention in the field of EMI shielding due to its extraordinary mechanical, thermal, electrical and chemical properties. The work described in this communication reignites further research to be done to establish GA as a next-generation effective EMI shielding material.

In the present investigation, GA was prepared using customised sol-gel polymerization chemistry. Initially, GO was synthesized by following rigorously the known synthesis protocol prescribed. It is being regularly prepared in our laboratory.[27] Briefly speaking first of all graphite oxide is prepared by following staudenmaier method. The graphite oxide was then repeatedly washed and dried. It was then subjected to thermal exfoliation by placing it in the pre-heated Furnace (at 1050 °C) under Ar atmosphere. The resulting material as verified by Raman and FTIR (Fig. S1 and S2) was GO. After that, GO was thoroughly dispersed in deionised water by using ultrasonication for 24 hours.The concentration of GO in water was 1 wt%. Further, resorcinol (R, 0.625 g), formaldehyde (F, 0.9 g) with sodium carbonate as a catalyst (C, 3 mg) were added to the GO suspension followed by magnetic stirring for 1.5 hours. Resorcinol and formaldehyde (RF solids) were 4 wt% of reactant concentration in the starting mixture. The molar ratio of R:C and R:F was 200:1 and 1:2, respectively. The final reaction mixture was poured into glass vials and cured in an oven at 85 °C (3 days) for gelation. Moreover, the wet cross linked gels were exchanged with acetone to extract water content present in the pores. Supercritical drying process was employed to dry wet gels using liquid CO_2. Finally, the carbonization was carried out at 900 °C for 3 hours under nitrogen ambient which yields the graphene aerogel. The details of the experiment performed (Fig.S3) together with locally fabricated supercritical dryer (Fig.S4) are given in supplementary information.

Structural characterization of the sample was done through X'Pert PRO (PANalytical) X-ray diffractometer equipped with a graphite monochromator utilizing CuKα_1 radiation (λ = 1.5406 Å). Fig. 1 (a) demonstrates the representative XRD pattern for the GA, which is showing a weak peak at 2Θ = 22.30° {this corresponds to (002 planes)} suggesting minimum stacking of (002) and larger interlayer spacing of the sheets. Moreover, there is a broad peak extending from 2Θ = 38 to 55°. This comes from (100)/(101) plane, which is consistent with other reports.[26] Representative Raman spectrum of GA taken using Horiba LabRAM HR800 (Argon LASER light of wavelength 514 nm) is shown in Fig. 1(b). It has intense D (1336 cm^{-1}) and G (1582 cm^{-1}) bands with broad 2D features, which are similar to the known Raman peaks for GA. The strong D band on the bulk graphene aerogel spectrum is probably because of the many junctions inbuilt in the 3D graphene network.[28] Fourier transform infrared spectroscopy (FTIR) was obtained by using a Perkin Elmer FTIR spectrometer (spectrum 100) in transmission mode in the wave number range 500 – 4000 cm^{-1}. FTIR spectrum of graphene aerogel is shown in Fig. 1 (c). The broad and strong peak near 3485 cm^{-1} indicates the stretching vibration of O-H bond. In addition, the peak at 1645 cm^{-1} can be attributed to the C=C stretching vibration. Peak around 1355 cm^{-1} result from the stretching vibrations of the C-O in the carboxyl group. The BET surface area was determined by the surface area analyzer (Micrometrics, USA, ASAP 2020 Models). Nitrogen porosimetry data indicates the textural properties of the graphene aerogel. Nitrogen adsorption/desorption isotherm {inset of Fig. 1 (d)}indicating that significant mesoporosity exists, which is consistent with the sheet-like structure observed in the electron micrographs. The actual BET surface area and pore volume of the graphene aerogel obtained is 516 m^2/g and 0.485725 cm^3/g, respectively. The pore size distribution {Fig. 1 (d)} shows that the peak pore diameter is ~ 2.5 nm which depends upon the RF polymer content in the initial precursor. DC conductivity of the GO and GA was determined via the four-point probe system (Keithley 6220 precision current source, Keithley 2182A Nanovoltmeter). Fig. 1(e) and 1(f) represents the room temperature I-V characteristics of GO and GA, respectively. The values of conductivities obtained for GO and GA samples are 85 S/m and 130 S/m, respectively. Here, it is found that GA has higher conductivity as compared with GO. This may be due to the reduction in the resistance at the junction between the graphene sheets.

Cite this: DOI: 10.1039/c0xx00000x

www.rsc.org/xxxxxx

ARTICLE TYPE

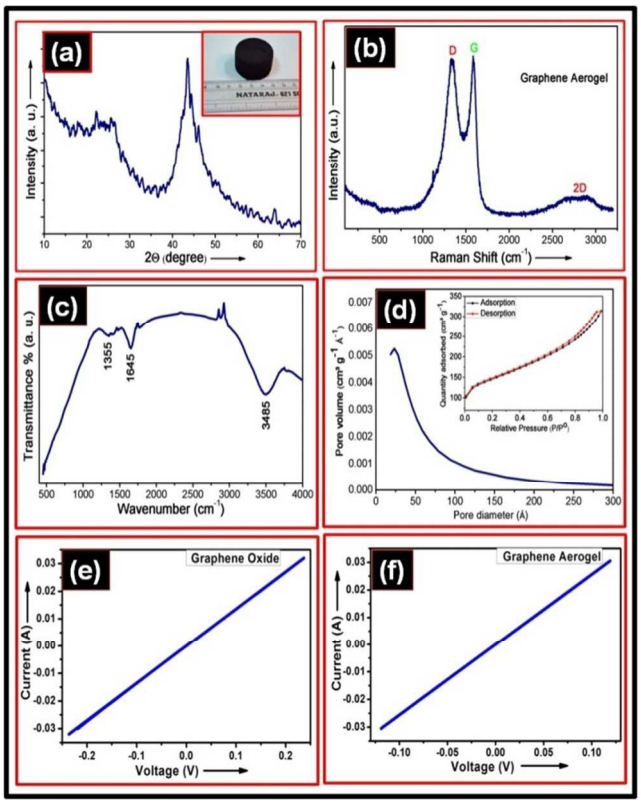

Fig. 1 a) XRD pattern of GA and inset is the optical image of GA, b) Raman spectrum of GA, c) FT-IR spectrum of GA, d) pore volume versus pore diameter graph at STP and inset is nitrogen adsorption/desorption isotherm, and e-f) I-V curve of GO and GA, respectively.

The surface morphological study of the as prepared GA was examined using scanning electron microscopy (SEM) {FEI, Quanta 200}. Figs. 2 (a) and (b) demonstrate the representative SEM micrographs of graphene aerogel at low and high magnification, respectively. It can be clearly seen that Fig. 2 (b) exhibits a 3D set of connections of randomly distributed sheet-like structures. These set of sheets are thin enough to be transparent to the electron beam. Microstructural characterization was performed by using FEI Technai-20 G^2 acceleration voltage (200 kV) high-resolution transmission electron microscope (HRTEM). A representative TEM and HRTEM micrographs of graphene aerogel is shown in Figs. 2 (c) and (d) at different magnification. TEM micrographs reveal a wrinkled paper-like texture to the sheets, which is consistent with previous studies.[29-30]

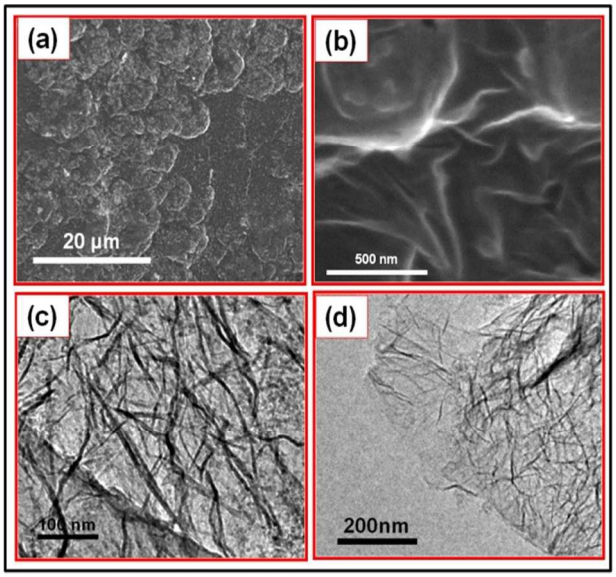

Fig. 2 Low and high magnification a) & b) SEM images and c) & d) TEM images of as prepared GA.

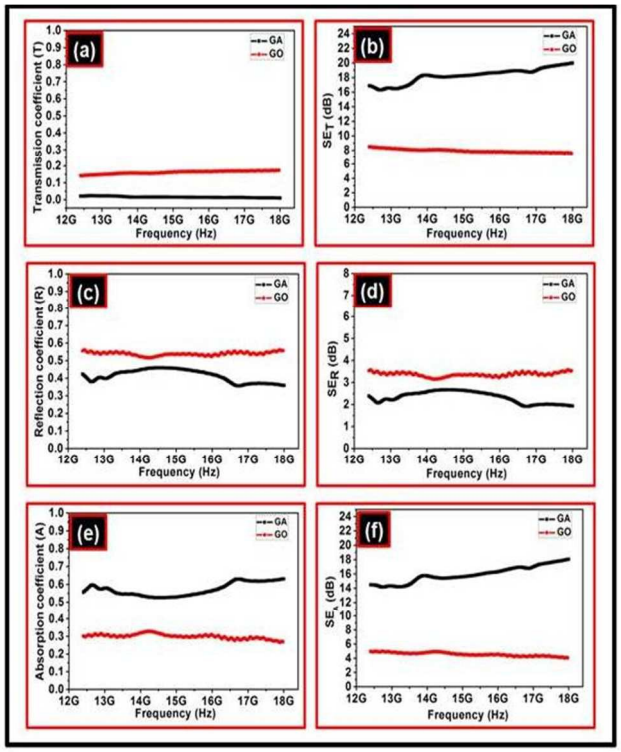

Fig. 3 a) Transmission (T), c) Refection (R), e) Absorption (A) coefficients and shielding effectiveness b) SE_T, d) SE_R, and f) SE_A of as synthesized GA as well as pristine GO in the frequency range of 12.4 - 18.0 GHz.

EMI shielding measurements were carried out on an Agilent E8362B vector network analyzer in the microwave range of 12.4–18.0 GHz. For this, the powder sample was pressed into a ~ 2 mm thick rectangular shaped pellet with a dimension to fit the waveguide dimensions. The EMI shielding effectiveness (SE) of a material is defined as the ratio of transmitted power to incident power and given by $SE_T(dB) = -10\log\{P_T / P_I\}$ where, P_I and P_T are the incident and transmitted power of EM waves, respectively. When an EM wave incident on the shield, it is partly absorbed, reflected and transmitted. Therefore, the total shielding effectiveness is the sum of shielding effectiveness due to reflection (SE_R), absorption (SE_A) and given by the expression $SE_T = SE_A + SE_R$. The scattering parameters S_{11} (or S_{22}) and S_{21} (or S_{12}) of a two port network analyzer can be related with reflectance and transmittance as, $T = |S_{21}|^2 = |S_{12}|^2$, $R = |S_{11}|^2 = |S_{22}|^2$.

The absorbance (A) can be written as $A = (1 - R - T)$. Here, it should be noted that the absorption coefficient is given with respect to the power of the incident EM wave. The relative intensity of the effectively incident EM wave inside the materials after first reflection is based upon the quantity (1-R). Therefore, the effective absorbance (A_{eff}) can be described as $A_{eff} = (1 - R - T)/(1 - R)$ with respect to the power of the effectively incident EM wave inside the shielding material. Therefore, it is convenient to express the reflection and effective absorption losses in the form of -10log (1-R) and -10log ($1-A_{eff}$) respectively, which give SE_R and SE_A as $SE_R = -10\log(1 - R)$ and $SE_A = -10\log(1 - A_{eff}) = -10\log(T/1 - R)$.

To show the excellent EM wave attenuation performances of the GA with changing frequency T (transmittance coefficient), R (reflection coefficient) and A (absorption coefficient) values were calculated and shown in Figs. 3 (a), (c) and (e). According to the plots as exhibited in Fig. 3 (e), the A values were in the range of 0.5 to 0.6 while the R values lied between 0.30 - 0.45. The T values are significantly small and lie within the range 0.008 - 0.024. Interestingly, T decreases with increasing frequency. Such small values show that the synthesized GA has potential shielding properties. In other words, due to higher A and R coefficient, more EM waves are consumed by GA. This leads significant decrease of T values. Figs. 3 (b, d & f) show the variation of the SE_T, SE_R, SE_A in the frequency range of 12.4 – 18.0 GHz. From the experimental measurement for GA, the shielding effectiveness due to absorption (SE_A) has been found to vary from ~ 14.5 to 18.0 dB while the SE_R varies ~ 1.9 to 2.3 dB for the same. Thus, the total SE_T achieved for the GA is ~ 20.0 dB, which is much higher than the pristine graphene oxide (GO) nanosheets. It is very interesting to note that GA is a better selection over conventional GO not only in the sense that it shows higher total SE but also SE_R is much less in GA as compared to GO. It has been observed that for GA, shielding effectiveness (SE) is mainly dominated by absorption while the shielding effectiveness due to reflection (SE_R) is almost constant, and it contributes negligibly.

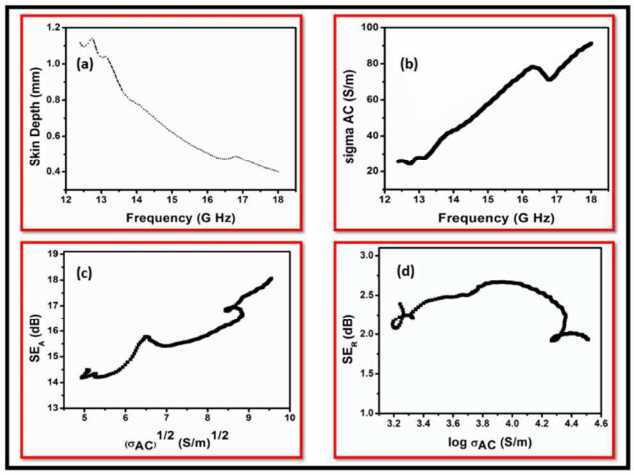

Fig. 4 a) Shows the plot of skin depth vs. frequency, b) variation of σ_{ac} with the increase in frequency, c) dependence of SE_A as a function of $(\sigma_{ac})^{1/2}$, d) variation of SE_R as a function of log σ_{ac} for graphene aerogel.

In order to understand the contribution of multiple reflections that are produced by the coupling of the reflected radiation on the first incidence plane and reflection in the final plane of the material, skin depth of the graphene aerogel shield have been evaluated using the relation $\delta = \sqrt{2/\omega\mu\sigma_{ac}}$ and its variation with frequency has been shown in Fig. 4 (a). The average skin depth of the graphene aerogel is found to be ~ 0.8 mm which is smaller than the thickness of the shield (2 mm). According to SchelKunoff's theory, multiple reflections can be neglected when the thickness of the shield is greater than the skin depth. Therefore, the term SE_M can be neglected. According to EM theory, for electrically thick samples (t > δ), frequency (ω) SE_R and SE_A can be expressed in the terms of conductivity (σ_{ac}) real permeability (μ'), skin depth (δ) and thickness (t) of the shield material as:

$$SE_R(dB) = 10\log\{\sigma_{ac}/16\omega\varepsilon_0\mu'\}$$

$$SE_A(dB) = 20\{t/\delta\}\log e = 20d\sqrt{\mu\omega\sigma_{ac}/2}\log e = 8.68\{t/\delta\}$$

The σ_{ac} can be related to the imaginary permittivity (ε") as $\sigma_{ac} = \omega\varepsilon_o\varepsilon"$ and its behavior has been shown in Fig. 4 (b). The variation of dielectric attributes (ε', ε") is shown in supplementary information (S5). To relate σ_{ac} with the shielding parameter of the material, SE_A has been plotted against $(\sigma_{ac})^{1/2}$, (Fig. 4 (c)). From the above equation, it is seen that better SE_A can be achieved from moderate conducting materials. The dependence of SE_R as a function of log σ_{ac} is shown in Fig. 4 (d). Therefore, to minimize SE due to reflection, moderate value of conductivity (σ_{ac}) is required.

Cite this: DOI: 10.1039/c0xx00000x

www.rsc.org/xxxxxx

ARTICLE TYPE

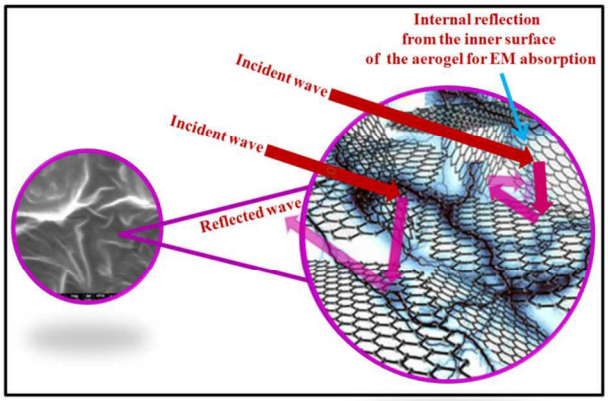

Fig. 5 Proposed mechanism of EMI shielding process through GA.

The plausible mechanism of EMI shielding through GA is shown in Fig. 5. The proposed reasons behind the observed SE are due to highly porous, light weight 3D sponge like structure of graphene aerogel, which provides the high surface area. The defects on the boundary of GA hinder the path of electrons, which contributes in dielectric losses and dissipates microwave energy. The dielectric losses occur in GA are the result of electronic, and space charges polarization. The contribution to the space-charge polarization appears due to the space charge accumulating at the interface of various layers leading to field distortion.

In conclusion, we demonstrate the microwave shielding properties of light weight 3D GA derived from graphene oxide (GO). The structural, microstructural and morphological characteristics of this nanostructure have been elucidated by XRD, SEM and TEM/HRTEM. The microstructural results clearly reveal that GA 3D architecture is composed of high-quality graphene layers with a very high surface area ~ 516 m^2/g. This engineered GA exhibit enhanced shielding effectiveness (~ 20.0 dB at 0.2 g in the frequency range 12.4 to 18.0 GHz) as compared to be conventional pristine GO. It has been found that GA improves the dielectric loss of GO which helps to increases the microwave shielding effectiveness in terms of its high microporosity (pore diameter ~ 2.5 nm), higher specific surface area, lower density and higher electrical conductivity. Moreover, the high microporosity of GA provides the better polarity along with good absorption capacity. Thus, the present result of EMI shielding of GA offers a new analogue of graphene in forms of GA. This could serve as a new material for next-generation EMI shielding applications.

Acknowledgements

The authors acknowledge MNRE (Mission mode project on Hydrogen Storage), DST, UGC and HWB (DAE), CMPDI (Ministry of coal) India for financial support. We would also like to thanks Prof. M. A. Worsley (Lawrence Livermore National Laboratory, USA) and Prof. A. S. K. Sinha (IIT, BHU) for helpful discussions.

Notes and references

[a]Nanoscience Centre, Department of Physics (Centre of Advanced Studies), Banaras Hindu University, Varanasi-221005, INDIA

[b]CSIR- National Physical Laboratory, New Delhi-110 012, India

*email address: heponsphy@gmail.com(O. N. Srivastava)

†Electronic Supplementary Information (ESI) available: Details of synthesis of GA and Locally fabricated Supercritical Dryer. see DOI: 10.1039/b000000x/

References

1 F. Qin and C. Brosseau, J. Appl. Phys., 2012, 111, 061301.

2 C. Y. Lee, H. G. Song, K. S. Jang, E. J. Oh, A. J. Epstein and J. Joo, Synth. Met., 1999, 102, 1346.

3 B. R. Kim, H. K. Lee, S. H. Park and H. K. Kim, Thin Solid Films., 2011, 519, 3492.

4 E. Ma, J. Li, N. Zhao, E. Liu, C. He, and C. Shi, Mater. Lett., 2013, 91, 209.

5 Y. Yang, M. C. Gupta, K. L. Dudley, R. W. Lawrence, Nano Lett., 2005, 5, 2131.

6 G. S. Wang, X. J. Zhang, Y. Z. Wei, S. He, L. Guo and M. S. Cao, J. Mater. Chem A 1., 2013, 7031.

7 B. Wen, M. Cao, Z. Hou, W. Song, L. Zhang, M. Lu, H. Jin, X. Fang, W. Wang and J. Yuan, Carbon, 2013, 65, 124.

8 Y. Qing, X. Wang, Y. Zhou, Z. Huang, F. Luo and W. Zhou, Compos. Sci. Technol., 2014, 102, 161.

9 W. Song, M. Cao, L. Fan, M. Lu, Y. Li, C. Wang and H. Ju, Carbon, 2014, 77, 130.

10 Y. Huang, Y. Wang, Z. Li, Z. Yang, C. Shen and C. He, J. Phys. Chem. C., 2014, 118, 26027.

11 D. Micheli, A. Vricella, R. Pastore and M. Marchetti, Carbon, 2014, 77, 756.

12 M. Cao, W. Song, Z. Hou, B. Wen and J. Yuan, Carbon, 2010, 48, 788.

13 B. Wu, H. M. Tuncer, A. Katsounaros, W. Wu, M. T. Cole, K. Ying, L. Zhang, W. I. Milne and Y. Hao, Carbon, 2014, 77, 814.

14 P. Tripathi, C. R. Prakash Patel, A. Dixit, A. P. Singh, P. Kumar, M. A. Shaz, R. Srivastava, G. Gupta, S. K. Dhawan, B. K. Gupta and O. N. Srivastava, RSC Adv., 2015, 5, 19074.

15 X. J. Zhang, G. S. Wang, W. Q. Cao, Y. Z. Wei, M. S. Cao and L. Guo, RSC Adv., 2014, 4, 19594.

16 D. Chen, G. S. Wang, S. He, J. Liu, L. Guo, and M. S. Cao, J. Mater. Chem. A 1., 2013, 5996.

17 M. Zong, Y. Huang, H. Wu, Y. Zhao, Q. Wang, and X. Sun, Mater. Lett., 2014, 114, 52.

18 P. B. Liu, Y. Huang, and X. Sun, ACS Appl. Mater. Interfaces., 2013, 5, 12355.

19 Y. Chen, G. Xiao, T. Wang, Q. Ouyang, L. Qi, Y. Ma, P. Gao, C. Zhu, M. Cao, and H. Jin, J. Phys. Chem. C., 2011, 115, 13603.

20 Y. Zhan, F. Meng, Y. Lei, R. Zhao, J. Zhong, and X. Liu, Mater. Lett., 2011, 65, 1737.

21 Y. Gao and Z. Tang, Small, 2011, 7, 2133.

22 Q. L. Liu, B. Cao, C. L. Feng, W. Zhang, S. M. Zhu, D. Zhang, Compos. Sci. Technol., 2012, 72, 1632.

23 F. Moglie, D. Micheli, S. Laurenzi, M. Marchetti, V. M. Primiani, Carbon, 2012, 50, 1972.

24 Z. Fang, C. Li, H. Sun, H. Zhang, J. Zhang, Carbon, 2007, 45, 2873.

25 H. B. Zhang , Q. Yan , W. G. Zheng , Z. X. He , Z. Z. Yu , ACS Appl. Mater. Interfaces., 2011 , *3* , 918 .

26 M. A. Worsley, T. T. Pham, A. M. Yan, S. J. Shin, J. R. I. Lee, M. Bagge-Hansen, W. Mickelson, A. Zettl, ACS Nano, 2014, 8, 11013.

27 M. S. L. Hudson, H. Raghubanshi, S. Awasthi, T. Sadhasivam, A. Bhatnager, S. Simizu, S. G. Sankar and O. N. Srivastava, Int. J. Hydrogen Energy., 2014, 39(16), 8311–8320.

28 P. J. Pauzauskie, M. A. Worsley, T. F. Baumann, J. H. Satcher, and J. Biener, U.S. patent., 2012, US 2012/0034442 A1.

29 M. J. McAllister, J. L. Li, D. H. Adamson, H. C. Schniepp, A. A. Abdala, J. Liu, M. Herrera-Alonso, D. L. Milius, R. Car, R. K. Prud'homme, I. A. Aksay, Chem. Mater., 2007, 19, 4396.

30 M. A. Worsley, P. J. Pauzauskie, T. Y. Olson, J. Biener, J. H. Satcher, and T. F. Baumann, J. AM. Chem. Soc., 2010, 132, 14067.

Graphical Table of Content

Facile synthesis of highly porous, light weight 3D sponge like graphene aerogel derived from graphene oxide for microwave shielding application.